Computational Fluid Dynamics of Reacting Flows at Surfaces: Methodologies and Applications

Daniele Micale[1], Claudio Ferroni[1], Riccardo Uglietti[1], Dr. Mauro Bracconi[1], Prof. Dr. Matteo Maestri[1,*]

In this review, we present the numerical algorithms and speed-up strategies developed to couple continuum macroscopic simulations and detailed microkinetic models in the context of multiscale approaches to chemical reactions engineering. CFD simulations and hierarchical approaches are discussed both for fixed and fluidized systems. The foundations of the methodologies are reviewed together with specific examples to show the applicability of the methods. These concepts play a pivotal role to enable the first-principles multiscale approach to systems of technological relevance.
Keywords: Chemical Reactors, Computational Fluid Dynamics, Hierarchical Modeling, Microkinetic Modeling, Multiscale Modeling

Author affiliations

[1]Politecnico di Milano, Laboratory of Catalysis and Catalytic Processes, Dipartimento di Energia, via La Masa 34, 20156 Milano, Italy
Email corresponding author: matteo.maestri@polimi.it

1   Introduction

Catalysis engineering has played a fundamental role in the chemical and energy industry in the past century. It enabled the industrial scale production of commodities and fuels, leading to a rapid progress of the society. Nowadays, new challenges have risen, mainly consisting of a sustainable exploitation of the raw material and energy consumption. In this view, this urges to develop more environmentally friendly and sustainable solutions, which represent a target of utmost significance to meet the Sustainable Development Goals posed by the United Nations.

In this context, the catalysis engineering is surely devoted to the research of new materials [1] aimed at activating novel reactions. In addition, the improvement of the currently existing technologies has a high significance to increase productivity, selectivity, and energy efficiency of the catalytic processes. To this aim, a computational modeling approach has been introduced to provide fundamental insights into the catalytic environment and to understand the complex intercoupling between the physical and chemical phenomena that influence the overall performances of the system. Indeed, the computational investigation can act as in silico experiments that allow for the analysis of systems without the need for the prior manufacturing of the reactor units.
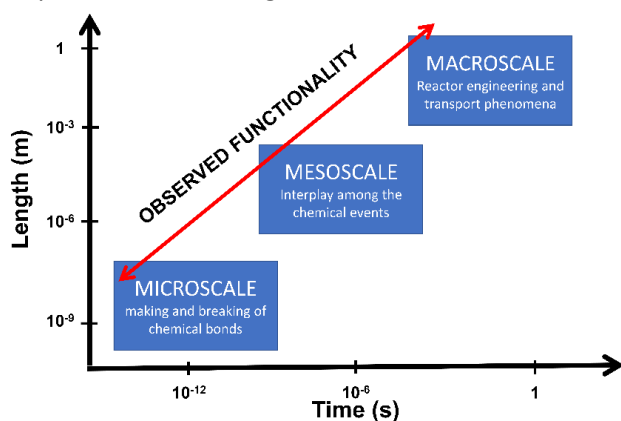

Figure 1. Schematic representation of the time and length scales involved in chemical processes. Adapted with permission from ref. [2].

A catalytic environment is characterized by phenomena occurring in a wide range of time and length scales, as schematized in **Figure 1**. The description of these phenomena and their interplay is challenging from a computational standpoint. In this view, the multiscale modeling approach can be adopted to tackle this challenge, by enabling the computational analysis of catalytic systems by accounting for the effects of all the phenomena [3,4]. In doing so, it allows for the quantitative investigation of such system by using a first-principles description of the phenomena. Accordingly, the different scales present in a catalytic environment are described by coupling the Computational Fluid Dynamics (CFD) predictions of the flow with the detailed descriptions of the chemical kinetics (i.e., mean fields microkinetics, kinetic Monte Carlo -kMC-), developed from the quantum mechanical electronic structural theory.

To this purpose, this review article aims at the critical discussion of the methods established to integrate detailed first-principles kinetic into the macroscale simulations, as presented in the plenary lecture at the Annual Meeting 2021 of the German Subject Group on Chemical Reaction Engineering [5]. First, the multiscale modeling approaches are presented with respect to fixed and fluidized reactors. Then, the numerical approaches available in the literature to perform the coupling between CFD and detailed descriptions of the chemical kinetic are discussed for each reactor class. In all the numerical strategies, the majority of the computational effort (i.e., 70-90%) is related to the solution of the chemistry, which requires expensive calculations and thus represents the bottleneck of the application of these approaches. In this context, different speed-up strategies have been developed in the literature to overcome such a limitation and they are hereby discussed. Despite the adoption of these techniques, the computational effort of the most detailed modeling approaches does not allow for their application for investigating industrial scale units or for routinely reactor analysis and design. As such, a hierarchical approach has been proposed to improve the accuracy of the medium or low detailed methodology by replacing the literature correlations, based on the empirical understanding of the phenomena, with correlations derived from data obtained by highly detailed simulations which account for the multiscale nature of the system.

2   Coupling CFD with the detailed description of chemical kinetic in catalytic reactors

In this section, the numerical methodologies for the coupling of CFD and detailed description of the gas-phase and surface reactivity are presented by separately discussing the approaches proposed for the description of fixed bed reactors (Section 2.1) and fluidized reactors (Section 2.2). For each system, the governing equations describing the evolution of the non-isothermal reactive flow in the reactor are initially discussed. Then, the numerical strategies needed to treat the reaction source terms are presented. These numerical strategies have been implemented in different numerical tools. Among them, Maestri and co-workers developed the catalyticFoam framework [6], a comprehensive tool for the first-principles multiscale investigation of catalytic reactors.

2.1 Fixed Bed Reactors

Catalytic fixed beds are key in the synthesis of many chemicals and intermediates and the abatement of pollutants and toxic substances [7–9]. To improve the existing reactor technologies and to develop novel processes, the fundamental investigation of the local flow structures present inside the reactor environment and their effects on the heat and mass transfer is required [10]. Consequently, since the late 1990s, the research has started focusing on developing methods to investigate fixed bed reactors by using CFD simulations to describe the complex 3D fluid dynamic of these units. In this context, two modeling approaches, characterized by a decreasing level of detail in the description of the geometrical complexity, have been proposed in the literature, namely, particle resolved [10,11] and porous media [12,13] models.

2.1.1 Particle Resolved Model

The particle resolved model is the most detailed strategy to investigate fixed bed reactors. Accordingly, the analysis of the reactor is performed by accounting for the actual geometry of the bed (**Figure 2** (a)).

In this view, the geometry of the solid phase must be computationally reconstructed [10,14,15]. Different approaches are present in the literature according to the catalytic system that has to be analyzed. In the case of packed beds, the virtual reconstruction is performed employing Discrete Element Method [16] (DEM) simulations [17–20] using commercial or open-source software packages (e.g., blender®, ligggths®, OpenFoam®). Conversely, the virtual reconstruction of a structured reactor can be performed by employing Computer-Aided Design (CAD) models in the case of regular structures [15,21–23] whereas DEM-based approaches can be used for irregular media, e.g., foams [14,24].

Then, the computational domain has to be obtained by means of a meshing procedure [10,25–28], which requires proper strategies to capture the complex morphology of the considered catalyst shape (e.g., bridges or caps in the case of packed bed reactors [25,29]). The meshing procedure also affects the phenomena described in the reactor environment. Indeed, only the phenomena with a characteristic length higher than the computational cell size can be accounted for in a particle resolved simulation. Hence, a fine mesh is needed if all the phenomena have to be properly described. However, the use of a fine mesh is often not feasible due to the high computational burden. In this view, coarse meshes are adopted and the governing equations are combined with closure models to account for the effects of the smallest scale phenomena (e.g., Reynold-Averaged Navier-Stokes in case of turbulent flow). Nevertheless, the computational grids usually adopted in this approach limits its applicability to small portions of the reactor environment. Hence, to properly describe and parametrically investigate the properties of interest, Representative Elementary Volumes (REV) of the catalytic reactor, sketched in **Figure 2** (b), must be chosen [15,30,31].

The particle resolved model has been used in the literature to describe all the different operating conditions present in a catalytic reactor [10,11] (e.g., chemical regime, internal mass and heat transport limitations, external mass and heat transport limitation). In particular, two modeling approaches can be found in the literature and will be discussed in the following sections.
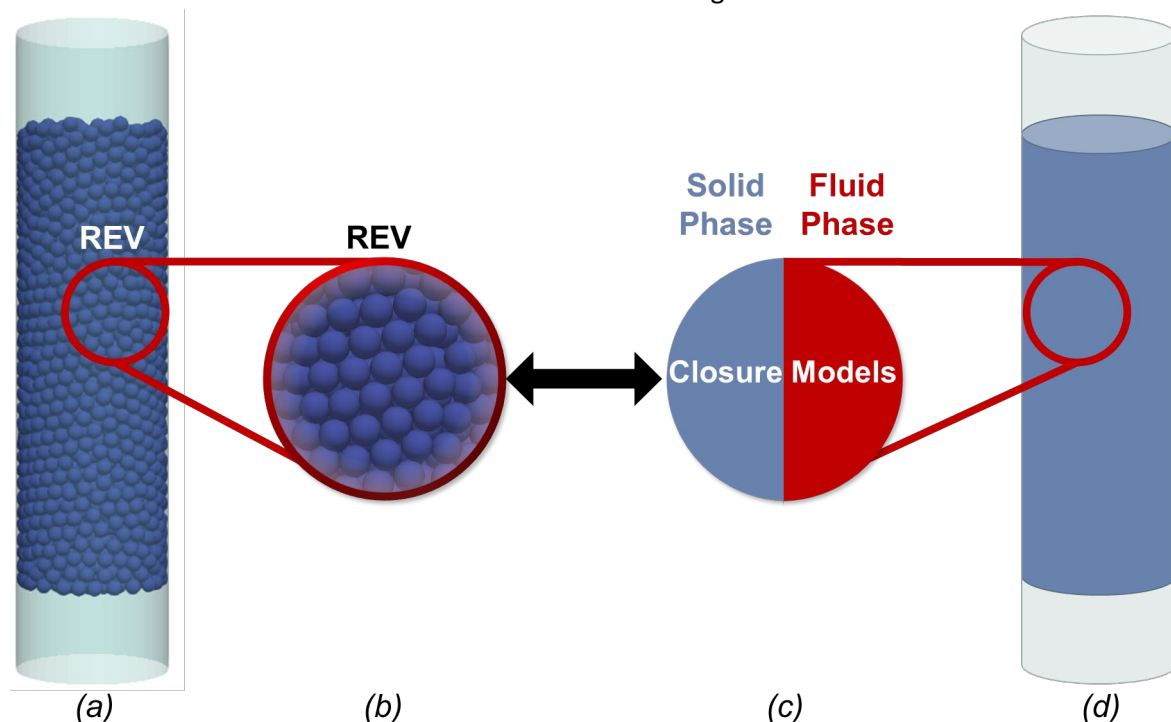

    (a)   *(b)*   *(c)*   *(d)*

Figure 2. Schematic representation of the fixed bed reactor and their Representative Elementary Volumes (REV) according to the particle resolved model (a)-(b) and the Volume Average Technique for porous media (c)-(d).

2.1.1.1 Single-region Particle Resolved Model

A single-region approach can be adopted to describe the fixed beds when the energy and species gradients inside the catalyst can be considered negligible. Hence, only the fluid region is meshed, since the presence of the catalytic material is introduced in the system as a boundary condition between the fluid phase and the solid walls.

In this approach, the fluid dynamic behavior of the units is predicted by solving the continuity and the Navier-Stokes equations (eqs. (1)-(2)) in the fluid phase computational domain.

$$\frac{\partial(\rho_f)}{\partial t} + \nabla(\rho_f \boldsymbol{U}_f) = 0 \tag{1}$$

$$\frac{\partial(\rho_f \boldsymbol{U}_f)}{\partial t} + \nabla(\rho_f \boldsymbol{U}_f \boldsymbol{U}_f) = -\nabla(p) + \rho_f \boldsymbol{g} + \nabla\left[\mu_f\left(\nabla \boldsymbol{U}_f + \nabla \boldsymbol{U}_f^T\right) - \frac{2}{3}\mu_f(\nabla \boldsymbol{U}_f)\boldsymbol{I}\right] \tag{2}$$

Moreover, the balance equations describing the evolution of the species (eq. (3)) and energy (eq. (4)) in the fluid have to be accounted for to describe non-isothermal reactive flows [6].

$$\frac{\partial(\rho_f \omega_{j,f})}{\partial t} + \nabla(\rho_f \omega_{j,f} \boldsymbol{U}_f) = -\nabla(\boldsymbol{J}_j) + R_j^{hom} \tag{3}$$

$$\rho_f \bar{c}_{p,f} \frac{\partial(T_f)}{\partial t} + \rho_f \bar{c}_{p,f} \boldsymbol{U}_f \nabla(T_f) = -\nabla(\boldsymbol{q}_{cond}) + Q^{hom} \tag{4}$$

In eqs. (3)-(4), proper closures are needed to model the diffusive and conductive fluxes, e.g., Fick (eq. (5)) and Fourier (eq. (6)) equations [32], respectively.

$$\boldsymbol{J}_j = \mathfrak{D}_j \nabla \omega_{f,j} \tag{5}$$

$$\boldsymbol{q}_{cond} = \lambda_f \nabla T_f \tag{6}$$

The catalytic material is introduced as boundary condition for the species (eq. (7)) and energy (eq. (8)). The heterogeneous reaction rate can be locally expressed as a function of the mean surface molar concentrations of fluid phase and adsorbed species, whose amount and variations are reported in eq. (9).

$$\rho_f \mathfrak{D}_j (\nabla \omega_{j,f})\big|_{catalyst} = \frac{A_{cat}^{eff}}{A} R_j^{het} \tag{7}$$

$$(\lambda_f \nabla T_f)\big|_{catalyst} = \frac{A_{cat}^{eff}}{A} Q^{het} \tag{8}$$

$$\frac{d\theta_k}{dt} = \frac{R_k^{het}}{\sigma_{cat}} \tag{9}$$

This approach is representative of systems operating in chemical regime or fully external mass and heat transfer limitations [6,15,31], and it has been successfully used to investigate the fluid dynamic and the reactivity of catalytic units working in laminar conditions [10]. The effect of internal transport limitations in the catalytic material can be included in this approach by considering an additional parameter (i.e., the effectiveness factor) [33–36]. However, this approach has been adopted only for systems with a thin catalyst layer [33,34] or with a single catalytic particle [35]. In addition, its combination with literature closure models aimed at introducing the effects of the turbulence in the fluid dynamic quantities enables also the investigation of turbulent and reactive units.

2.1.1.2 Multi-region Particle Resolved Model

The investigation of intra-phase mass and heat transfer resistances can be performed by adopting a single-region approach only for systems which allow for an accurate evaluation of the effectiveness factor. To describe in a more general way these phenomena, the characterization of the species and temperature distribution inside the pellets and their relation with the properties of the catalyst porous matrix (e.g., porosity, tortuosity, pore size distribution) is mandatory. In this context, a multi-region approach has to be used to describe the catalytic environment. Accordingly, the solid phase is modeled as a pseudo-homogeneous phase, thus adopting effective transport properties [37] to account for the internal porous

structure of the catalyst. Different closures have been developed in the literature to derive the effective transport properties (e.g., ε/τ model, Wakao-Smith model) [33]. They aim at correcting the molecular gas diffusivity by accounting characteristic of the catalytic porous matrix. Hence, analysis of the internal catalyst structures has been performed to properly quantify these properties [38,39] and effectively adopt the aforementioned models. In doing so, the computational domain is composed of two meshes, one for the fluid and a second for the catalytic material, sharing the fluid-solid interface. Proper boundary conditions are here imposed to enable the communication between the two domains and, usually, a consistent meshing approach is adopted [37].

In this approach, the fluid phase is solved analogously to the single-region approach (eqs. (1)-(4)). However, the governing equations of the solid phase (eqs. (9)-(11)) have to be accounted for the description of the species and energy transport in the catalytic particles. In contrast, the Navier-Stokes equations are not solved in the solid phase since the absence of a convective flow is assumed. Hence, constant pressure and a null fluid velocity characterize the solid phase [37].

$$\frac{\partial(\rho_{f,s}\omega_{j,s})}{\partial t} = \nabla(\rho_{f,s}\mathfrak{D}_j^{\text{eff}}\nabla\omega_{j,s}) + R_j^{het} \tag{10}$$

$$(\rho_s(1-\kappa_s)c_{p,s} + \rho_{f,s}\kappa_s\bar{c}_{p,s})\frac{\partial T_s}{\partial t} = \nabla(\lambda_f^{eff}\nabla T_s) + Q^{het} \tag{11}$$

In this approach, the gas-solid boundary condition is key to enable the communication between the two regions. In particular, it is important to ensure that the flux of species or energy from the fluid to the interface is equal to the flux from the interface to the solid catalyst to avoid an unphysical accumulation of energy or species at the gas-solid interface. Moreover, it is also mandatory that the temperature and species composition of both the computational domains must be equal at the fluid-solid interface. This coupling condition translates into eqs. (12)-(13) (energy boundary condition) and eqs. (14)-(15) (species boundary condition) imposed at the interface between the fluid and solid phase.

$$-\lambda_f\nabla T_f = -\lambda_{eff}\nabla T_s \tag{12}$$

$$T_f^I = T_s^I \tag{13}$$

$$-\rho_f\mathfrak{D}_j \nabla\omega_{j,f} = -\rho_{f,s}\mathfrak{D}_j^{\text{eff}}\nabla\omega_{j,s} \tag{14}$$

$$\omega_{j,f}^I = \omega_{j,s}^I \tag{15}$$

This modeling approach has been successfully adopted to analyze reactors with intra-phase mass and heat transfer resistances [10,37]. However, this description is obtained with a higher computational cost with respect to the single-region one. Indeed, two meshes must be solved and the governing equations of the solid phase (eqs. (9)-(11)) are not accounted for only at the fluid-solid interface (single-region approach) but they are solved for each solid computational cell, leading to a relevant increment of the computational effort.

2.1.2 Porous Media Model

The application of the particle resolved model is hampered by its computational cost, and thus it can be exploited to investigate only a small portion of the reactor (e.g., few hundreds/thousands of particles in case of packed beds or unitary cells in the case of cellular materials) [15,30,31]. Consequently, a more computational affordable numerical strategy is needed to enable the analysis of industrial-sized units.

To do so, the Volume-Averaging Technique (VAT), originally introduced by Whitaker [12,13], is employed for the description of the solid and the fluid phase and their mutual interactions. A schematic representation of the VAT is reported in **Figure 2**(c)-(d). The purpose of the VAT is to treat a complex fluid-solid system (**Figure 2** *(a)*) by completely disregarding its geometry, which is accounted for by means of simplified engineering correlations for the geometrical and transport properties. In doing so, the information related to the three-dimensional and complex morphology of the porous medium (**Figure 2** *(a)*) is lost, and only the macroscopical effect of the catalyst on the reacting flow are obtained (**Figure 2**

(d)). In this view, similar approaches have been often adopted in the literature to simplify the transport phenomena inside complex systems [40,41]. Conversely, the implementation of the VAT in the catalyticFoam framework enabled the coupling between the fluid dynamics description with the detailed chemical kinetics with a multi-region approach. The solid phase of the catalyst is treated by means of a separate computational domain, topologically matching the corresponding fluid phase of the porous medium, where the evolution of the mean local average coverage, species and temperature in the catalyst is described as a function of the heterogeneous reaction rates. Then, the composition of the fluid phase is updated accounting for the fluid-solid inter-phase transport. Additionally, it allows for considering multiple porous regions and to account for the effect of different catalysts shape (e.g., particles or structured catalysts) on the average fluid dynamic conditions by means of closure models which retain micro- and meso-scale information. In this view, closure models can be developed based on the fundamental information acquired by means of detailed, particle-resolved approaches. Hence, the VAT for porous media is a medium hierarchy model based on the outcomes obtained by the high hierarchy approach (i.e., particle resolved).

The VAT is thus employed to simplify the governing equations which are valid within each phase of the porous medium (solid, fluid) to equations that are valid everywhere in the porous medium (**Figure 2** *(d)*) [12,13]. To begin with, the method of volume averaging is discussed for the continuity equation and the Navier-Stokes equation:

$$\frac{\partial \hat{\rho}_f}{\partial t} + \nabla(\hat{\rho}_f \boldsymbol{U_f}) = 0 \tag{16}$$

$$\frac{\partial(\hat{\rho}_f \boldsymbol{U_f})}{\partial t} + \nabla(\hat{\rho}_f \boldsymbol{U_f} \boldsymbol{U_f}) = -\nabla(\hat{p}) + \nabla(\hat{\mu}_f \nabla \boldsymbol{U_f}) + \Pi \tag{17}$$

where the accent ˆ denotes the spatially-averaged variables [12,13] and $\prod$ is a pressure source term. In this view, $\prod$ is a function of the geometry of the considered porous medium and the fluid transport properties and velocity, and is given by engineering correlations [42–45]

The VAT was extended enabling the solution of the Navier-Stokes in the chemical reactor coupled with the solution of the chemical species mass balance and the enthalpy balance in the porous medium. To do so, the fluid and the solid phases are treated separately as two different regions (fluid region, solid region, i.e., multi-region approach). In the fluid region, the species mass balance (eq. (18)) and the energy balance (eq. (20)) are required as governing equations, and the species and energy sources are evaluated by means of engineering correlations as reported in eqs. (19) and (21) respectively.

$$\frac{\partial(\hat{\rho}\hat{\omega}_{f,j})}{\partial t} + \nabla(\hat{\rho}\hat{\omega}_{f,j}\boldsymbol{U_f}) = \nabla(\mathfrak{D}_j \nabla \hat{\omega}_{f,j}) + S\omega_j^{f \to s} \tag{18}$$

$$S\omega_j^{f \to s} = \frac{Sh_j \mathfrak{D}_j}{L_{char}} S_v(\hat{\omega}_{s,j} - \hat{\omega}_{f,j}) \tag{19}$$

$$\hat{\rho}_f \hat{c}_{p,f} \frac{\partial(\hat{T}_f)}{\partial t} + \hat{\rho}_f \hat{c}_{p,f} \boldsymbol{U_f} \nabla(\hat{T}_f) = \nabla(\hat{\lambda}_f \nabla \hat{T}_f) + \Psi^{f \to s} \tag{20}$$

$$\Psi^{f \to s} = \frac{Nu \cdot k_f}{L_{char}} S_v(\hat{T}_s - \hat{T}_f) \tag{21}$$

In the solid region, the species mass balance (eq. (22)), the energy balance (eq. (23)), and the evolution of surface coverage (eq. (24)) are required as governing equations.

$$R_j(\hat{\omega}_{s,j}) - S\omega_j^{f \to s} = 0 \tag{22}$$

$$\hat{\rho}_s c_{p,s} \frac{\partial(\hat{T}_s)}{\partial t} = \nabla(\lambda_{eff} \nabla \hat{T}_s) - \Psi^{f \to s} + Q^{het} \tag{23}$$

$$\frac{\partial \hat{\theta}_{k,s}}{\partial t} = \frac{R_k^{het}}{\sigma_{cat}} \tag{24}$$

It is worth noticing that the accumulation term of the energy balance on the solid (eq. (23)) is considered to capture the dynamic evolution of the solid phase temperature. On the contrary, with respect to chemistry, eq. (22) is obtained with the assumption that local steady-state conditions are achieved. Thus,

the interphase transfer rate of the j-th species is always equal to the reaction rate. In this view, similarly to $\prod$, the Sherwood and Nusselt numbers and the effective thermal conductivity are quantified with engineering correlations, which are a function of the geometry of the considered porous medium and the fluid transport properties and velocity [15,30,31,42,46].

2.1.3 Numerical Strategies

The particle resolved and the porous media models can be equally simulated by means of either steady-state or transient solvers depending on the target of the investigations. The governing equations that characterize both the two approaches represent a set of Partial Differential Equations (PDE) with stiff and non-linear terms. Their solution in complex geometries with detailed kinetic mechanisms represents a challenging problem [6]. Indeed, the high stiffness and non-linearity of the chemical terms require efficient and robust numerical algorithms to be solved.

A fully segregated approach, efficiently applied to simulate non-reacting flows [10], cannot be used in this context since it is not effective to treat stiff and non-linear systems [47]. Similarly, the fully coupled solution of these equations [48] cannot be performed since the resulting systems of governing equations can be extremally large [6]. Thus, different algorithms based on the segregated approach with specific methods for the management of the reaction source terms have been developed in the literature to treat these systems achieving an effective methodology for the solution of the numerical problem.

2.1.3.1 Operator Splitting Method

The Operator Splitting (OS) [49] is a numerical strategy developed to efficiently treat sets of PDEs containing non-linear terms. According to this approach, the equations are solved by decoupling their constitutive terms to employ the optimal solution strategy for each of them. The OS has been successfully used in different research fields (e.g., combustion [50], atmospheric modeling [51]). Consequently, it has been also used to couple the detailed description of the homogeneous and heterogeneous chemical kinetic with the CFD solution of the complex flow in fixed bed reactors, and thus it represents the main approach to treat transient simulations with both single- or multi-region descriptions of the catalytic environment. As such, the solution of the governing equation is performed by decoupling the advection terms from the one related to the chemistry and by solving them sequentially.

By considering a generic variable φ whose evolution is determined by eq. (25), its solution is obtained in three steps according to the Strang algorithm [52].

$$\frac{\partial \varphi}{\partial t} = M(t) + S(t) \tag{25}$$

In the first step, called transport step, only the advective contributions $M(t)$ of the governing equations are accounted for the evolution of the thermo-chemical composition of the computational domain (eq. (26)).

$$\frac{\partial \varphi}{\partial t} = M(t) \tag{26}$$

Consequently, a fully segregated solution of the equation can be accurately performed by adopting linear matricial solvers since the resulting set of equations is non-stiff (because the reaction term is ignored). This step is solved over one half of the time step, and it is performed to first update the cell composition and temperature. The new composition and temperature become the initial conditions for the next sub-step.

Then, the reaction terms, ignored in the first step, are considered in the second one, called reaction step (eq. (27)).

$$\frac{d\varphi}{dt} = S(t) \tag{27}$$

In this step, each computational cell is described as a batch reactor and thus, its solution can be obtained through an Ordinary Differential Equation (ODE) solver. This is able to accurately manage the stiffness and non-linearity of the reaction source terms allowing for the correct description of the dynamic evolution

of the system. This step is solved along the whole simulation time step to provide a second update of the thermo-chemical composition over the domain which becomes initial conditions for the final step.

At last, the final condition on each computational cell is achieved by solving the transport step (eq. (26)) similarly to the first one with the exception that the initial conditions correspond to the final state of the second step.

This numerical strategy has been successfully applied in the literature to simulate the dynamic evolution of fixed bed reactors. In particular, a packed bed reactor of Raschig rings [6] and a packed bed reactor of porous spheres [37] have been successfully simulated using the single-region and the multi-region particle resolved model respectively, by adopting a UBI-QEP microkinetic scheme for the combustion of hydrogen on Rh [53]. However, it cannot be used if the investigation of the catalytic environment is performed with steady-state solvers.

2.1.3.2 Linearization of the Reactive Source Terms

In the literature, different approaches have been developed to solve the non-isothermal reactive flow by means of steady-state solvers. The main approach exploited in the multi-region description of the reactive environment involves the linearization of the reaction source terms (LRS). By adopting this approximation, the non-linearity of the species and the energy balance equation is neglected. Consequently, the solution of those equations can be achieved by adopting a fully segregated approach where the adsorbed species are, however, computed through a fully coupled method to guarantee a coverage that is consistent to the local bulk phase condition. To do so, a First Order Taylor expansion is adopted in literature to approximate the non-linear rates of the gas-phase species related to both homogeneous and heterogeneous reaction by neglecting the off-diagonal terms of the Jacobian matrix:

$$R_j^{hom/het} = R_{j,0}^{hom/het} + \frac{dR_j^{hom/het}}{d\omega_{j,f/s}}\Bigg|_0 (\omega_{j,f/s} - \omega_{j,0,f/s}) \tag{28}$$

In the context of homogeneous reactions, this approach can be efficiently exploited for all the modeling approaches previously described (i.e., particle resolved and porous media). Conversely to the homogeneous reactions, the LRS can be exploited to solve the heterogeneous chemical kinetic only if a multi-region description of the system is adopted (i.e., multi-region particle resolved model, porous media model), since a computational domain where the governing equations are discretized is mandatory to adopt this numerical strategy. Indeed, it has been successfully adopted to investigate the steady-state conditions of a packed bed reactor under steam reforming reacting conditions [54].

2.1.3.3 Reactive Source Terms as Boundary Condition

A proper approach is required to achieve the steady-state solution of the solid phase governing equations in the single-region approach. In this context, the Reactive Source Terms introduced in the form of Boundary condition (RSBC) provides satisfactory results. In addition, this approach can be also adopted to describe the transient behavior of fixed bed units with a more affordable computational cost. In contrast to the OS approach, the RSBC can be effectively used only in peculiar cases, i.e., systems whose reactivity is described by means of poorly stiff kinetics or working in external mass transfer limited regime. Accordingly, the update of the adsorbed species is achieved by solving the eq. (9) with an ODE solver. The obtained solution in terms of coverages is then exploited to evaluate the heterogeneous reaction source terms of the fluid phase species (R_j^{het}) required to impose the reactive boundary conditions (eqs. (7)-(8)). In doing so, the thermo-chemical composition of the gas phase can be computed with a fully segregated approach by considering the reactive boundaries as a material and heat flux. The RSBC has been successfully employed for the fundamental investigation of the transport properties of structured reactors (e.g., Foam [31] and Periodic Open Cellular Structures -POCS [15]).

2.2 Fluidized systems

Fluidized reactors are units in which the catalytic particles continuously change their position due to the interactions between them and with the fluid phase. For these units, the simplified 1D modeling approaches [55] are not able to describe the different flow structures (e.g., bubbles, clusters of particles) present in the reactor environment. Consequently, CFD approaches are used in the literature to analyze the complex 3D fluid dynamics of fluidized reactors. In particular, three different approaches have been proposed to predict the fluid dynamic of the multiphase flow: Direct Numerical Simulation (DNS) [56], Euler-Lagrange model [57–59], and Euler-Euler model [60,61]. These approaches differ for the level of details of the multiphase flow description and consequently, they can be applied to systems of different sizes.

2.2.1 Direct Numerical Simulation

The DNS is a numerical approach that describes in detail all the interactions between the gas and solid particles. Hence, the size of the computational cells of the domain must be chosen smaller than the particle diameter in this strategy. Each particle is tracked by solving the Newton's equation of motion. For what concerns the CFD solution of the gas phase, instead, the Immersed Boundary Method [56] is used. Accordingly, the computational grid is not rebuilt at each time step, despite the solid phase movement. Indeed, the surface of each particle is discretized and tracked by means of an ensemble of Lagrangian points. By doing so, the pressure and velocity fields are described until the gas-particle interface, and the gas-particle forces are directly obtained from the solution of the CFD governing equations, without the application of additional closure models. Despite the high level of detail of DNS simulations, the required computational cost limits the application of this approach to few hundreds of particles [56]. Thus, the Euler-Lagrange and Euler-Euler models are usually adopted for the modeling of the gas-solid flow from lab to industrial fluidized beds.

2.2.2 Euler-Lagrange Model

According to the Euler-Lagrange model, the gas phase is solved by means of CFD governing equations (eqs. (29)-(30)) while the evolution of the solid phase is obtained by tracking each particle in the domain as a moving material point (eq. (31)) across computational cells, which are 2-5 times bigger than the tracked particles [62].

$$\frac{\partial(\varepsilon \rho_f)}{\partial t} + \nabla(\varepsilon \rho_f \boldsymbol{U}_f) = 0 \tag{29}$$

$$\frac{\partial(\varepsilon \rho_f \boldsymbol{U}_f)}{\partial t} + \nabla(\varepsilon \rho_f \boldsymbol{U}_f \boldsymbol{U}_f) = -\varepsilon \nabla(p) + \varepsilon \rho_f \boldsymbol{g} + \nabla(\bar{\bar{\boldsymbol{\tau}}}_f) + \boldsymbol{F}^{f \to s} \tag{30}$$

$$m_p \frac{d\boldsymbol{U}_p}{dt} = m_p \boldsymbol{g} + \boldsymbol{F}_{d,p} + \boldsymbol{F}_{b,p} + \boldsymbol{F}_{coll,p} \tag{31}$$

Differently from the DNS, this numerical method has been adopted in literature to investigate reactive fluidized units [27,63–66]. A cell-wise solution of the heterogeneous reactivity is usually employed in the literature [67]. However, this approach does not account for the presence of possible interphase transport limitations. Thus, it does not allow for the multiscale investigation of the reactive environment since it is not able to catch all the phenomena occurring in the system. Consequently, the particle tracking approach has been extended to treat detailed chemistries by implementing the species and energy governing equations for both the fluid and each particle composing the solid phase together with the balance equations describing the evolution of the adsorbed species in each solid entity [63].

The species and energy balance equations for the fluid phase are reported in eqs. (32)-(33).

$$\frac{\partial(\varepsilon \rho_f \omega_{j,f})}{\partial t} + \nabla(\varepsilon \rho_f \omega_{j,f} \boldsymbol{U}_f) = -\nabla(\varepsilon \boldsymbol{J}_j) + R_j^{hom} + S\omega_j^{f \to s} \tag{32}$$

$$\varepsilon \rho_f c_{p,f} \frac{\partial(T_f)}{\partial t} + \varepsilon \rho_f c_{p,f} \boldsymbol{U}_f \nabla(T_f) = -\nabla(\varepsilon \boldsymbol{q_{cond}}) + \Psi^{f \to s} + Q^{hom} \tag{33}$$

The $S\omega_j^{f\to s}$ and $\Psi^{f\to s}$ retain the information of the coupling between the fluid and the solid phase and their evaluation depends on the modeling assumption adopted to describe the solid phase. In particular, according to the Lagrangian approach, $S\omega_j^{f\to s}$ and $\Psi^{f\to s}$ are evaluated by summing the terms calculated for each solid particle present in the computational cell.

The species (eq. (34)), the energy (eq. (35)) and the adsorbed species (eq. (36)) balance equations for the solid phase, solved for each solid entity present in the system, are hereby reported.

$$\frac{d(\rho_{f,p}\kappa_s\omega_{j,p})}{dt} = -Kc_jS_v\bar{\rho}(\omega_{j,p} - \omega_{j,f}) + R_j^{het} \tag{34}$$

$$(1-\kappa_s)\rho_p c_{p,p}\frac{dT_p}{dt} = -hS_v(T_p - T_f) + Q^{het} \tag{35}$$

$$\frac{d\theta_{k,p}}{dt} = \frac{R_k^{het}}{\sigma_{cat}} \tag{36}$$

The Euler-Lagrange model has been successfully used in the literature to investigate system up to the lab-scale [27,63–66]. Representative parcel models (i.e., coarse-graining method) [68,69] have been proposed to increase the size of the domain (i.e. number of particles). This is achieved by assembling a certain number of particles in a computational parcel in order to reduce the solid entities that have to be tracked. However, it is not applicable to industrial units, characterized by billions of particles, due to computational effort related to the particle tracking. In this view, the Euler-Euler model can be used to describe fluidized units till the industrial scale.

2.2.3 Euler-Euler Model

The Euler-Euler model overcomes the computational burden of the tracking cost, allowing the description of industrial scale reactors, by solving the solid phase as a fluid-like phase. Thus, it treats both the fluid and the solid phases as a continuum which appear as two interpenetrating fluids, removing the dependency of the computational cost on the number of particles present in the system. Consequently, the gas phase is solved coherently to the Euler-Lagrange model (eqs. (29)-(30)), while the solid phase loses its discrete nature and its fluid dynamics is predicted through the continuity and Navier–Stokes equations (eqs. (37)-(38)).

$$\frac{\partial((1-\varepsilon)\rho_s)}{\partial t} + \nabla((1-\varepsilon)\rho_s\boldsymbol{U_s}) = 0 \tag{37}$$

$$\frac{\partial((1-\varepsilon)\rho_s\boldsymbol{U_s})}{\partial t} + \nabla((1-\varepsilon)\rho_s\boldsymbol{U_s}\boldsymbol{U_s}) = -(1-\varepsilon)\nabla(p) + (1-\varepsilon)\rho_s\boldsymbol{g} + \nabla(\bar{\bar{\boldsymbol{\tau}}}_s) - \boldsymbol{F}^{f\to s} \tag{38}$$

This involves the adoption of additional closure models needed to describe the fluid properties of the solid phase, such as the Kinetic Theory of Granular Flow (KTGF) [60]. The KTGF requires that a statistically relevant number of particles is contained inside a computational cell to accurately predict the continuum behavior of the solid phase. Thus, a computational grid size ten times larger than the particle diameter is usually adopted in this modeling approach [60]. In literature, the Eulerian-Eulerian description has been successfully exploited to simulate the fluid dynamic of different kinds of fluidized units [70–73]. Then, it was extended to treat also non-isothermal reacting flows [70,74–77]. In doing so, the solution of the species and energy balance equations for both the fluid and the solid phases together with the adsorbed species balance equations for the solid phase are introduced in the framework.

Coherently with the Euler-Lagrange model, the species and energy balance equations for the fluid phase are formulated as reported in eqs. (32)-(33). However, $S\omega_j$ and $\Psi^{f\to s}$ are evaluated by considering the average properties of the solid phase since a fluid-like description of the solid phase is adopted in the Euler-Euler model.

The species and energy balances and the coverage balance equations are expressed as reported in eqs. (39)-(41) respectively.

$$\frac{\partial(\kappa_s(1-\varepsilon)\rho_{f,s}\omega_{j,s})}{\partial t} + \nabla(\kappa_s(1-\varepsilon)\rho_{f,s}\omega_{j,s}\boldsymbol{U_s}) = R_j^{het} - S\omega_j^{f\to s} \tag{39}$$

$$(1 - \kappa_s)(1 - \varepsilon)\rho_s c_{p,s}\frac{\partial(T_s)}{\partial t} + (1 - \varepsilon)\rho_s c_{p,s}\boldsymbol{U_s}\nabla(T_s)$$
$$= -\nabla \cdot ((1 - \varepsilon)\boldsymbol{q_{cond}}) - \Psi^{f\rightarrow s} + Q^{het} \tag{40}$$

$$\frac{\partial\theta_{k,s}}{\partial t} + \nabla(\theta_{k,s}\boldsymbol{U_s}) = \frac{R_k^{het}}{\sigma_{cat}} \tag{41}$$

In eqs. (39)-(41), there are additional contributions with respect to the Euler-Lagrange formulations (eqs. (34)-(36)) which represent the convection of species, temperature, and adsorbed species in the solid phase, which are mandatory since the discrete nature of the solid is lost. Additionally, no diffusive transport is considered in the solid due to the granular nature of this phase [75–77].

2.2.4 Numerical Strategies

In the context of fluidized units, steady-state solvers cannot be used because of their intrinsic dynamic evolution, thus, only transient solvers are adopted for their description. Moreover, the multiscale description of the reactive flow introduces strong non-linear terms in the energy, species, and adsorbed species balance equations related to the homogeneous and heterogeneous reaction source terms. Thus, proper numerical strategies have been developed in the literature to solve this set of PDE with non-linear terms. A fully coupled approach [48] cannot be adopted also in the case of fluidized units. Consequently, different approaches based on the segregated one have been exploited to treat the reactivity in these systems.

2.2.4.1 Constant and Linearized Reaction Source Terms

The most common approach in the literature to include the chemical kinetic in reactive simulations of fluidized systems [70,74,75] is the LRS. Coherently with the approach used in steady-state simulations of fixed bed reactor, the LRS involves the segregated solution of all the variables by linearizing the homogeneous and heterogeneous reactions source terms by means of a first-order Taylor expansion, eq. (28). In doing so, very small simulation time steps (i.e., below 10^{-6} s) are required to catch the transient behavior of the reactor, in particular when a detailed description of the chemical kinetic is used [78]. Thus, the LRS limits the computational performance of the approach previously described. This approach has been improved in literature by substituting the linearized reaction source term with a constant value computed by averaging over the time step the rigorous integration of the reaction rates [76]. However, also in this case, the segregated solution of the variables requires small time steps to avoid numerical errors, leading to a strategy that is still not able to manage the chemical kinetics along with the whole dynamic of industrial units. Consequently, different modeling approaches have been developed in the literature to increase the efficiency of the multiscale modeling approaches for fluidized units.

2.2.4.2 Multiphase Operator Splitting Method

The Multiphase Operator Splitting (MOS) [77], schematized in **Figure 3**, has been developed to overcome the issues highlighted in the aforementioned strategies to treat the reactive multiphase flows. Accordingly, the governing equations are solved in two sequential steps.
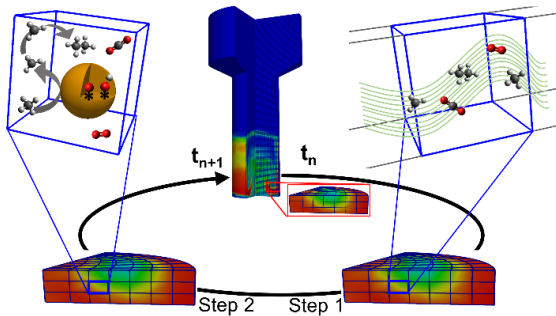
Figure 3. Schematic representation of the Multiphase Operator Splitting numerical strategy. Adapted with permission from ref. [77]. Copyright 2021 American Chemical Society

In the first step, the advection terms are considered in the solution of the governing equations of both the gas and the solid phase. In doing so, the segregated approach allows for the solution of these PDEs by means of a linear matricial solver since the challenging non-linear terms are absent.

Then, the compositions have been adopted as initial conditions for the second step, where the homogeneous and heterogeneous reactions and the interphase transport are accounted for. In doing so, each computational cell appears as a multiphase batch reactor that can be efficiently solved using an ODE solver since only local terms are present. In particular, the ODE solver can treat the stiffness and non-linearity of the reaction source terms and it allows for the coupled solution of the fluid and solid phases.

In doing so, the time splitting of the phenomena proposed by the MOS leads to a solution only slightly dependent on the time step [77], since the segregation of the strongly coupled phenomena is not performed. Consequently, this numerical approach allows to perform the reactive simulations with the same Courant conditions of the non-reactive ones enabling the management of detailed description of the chemical kinetic along with the whole dynamic of industrial units by adopting a Eulerian-Eulerian description of the multiphase flow. Indeed, it has been efficiently exploited to simulate an industrial fluidized bed reactor whose reactivity is described by a complex homo-hetero microkinetic mechanism of the OCM processes [79–81].

2.2.4.3 Operator Coupling Method

By considering a Lagrangian approach, the MOS cannot be adopted since the coupling between the computational cell and all the particles thereby contained will result in an extremely large system of governing equations. Consequently, in the Euler-Lagrange approach different numerical strategies have been developed to treat in a fully segregated way the gas and the solid phases.

In these strategies, the solution of the fluid phase governing equations can be achieved coherently with the approaches described for fixed bed reactors (i.e. LRS or OS).

Conversely, on the solid phase standpoint, the most rigorous approach that can be adopted to solve eqs. (34)-(35) is the Operator Coupling (OC), sketched in the left branch of **Figure 4**. Accordingly, the thermo-chemical composition of a solid particle is computed by solving the evolution of the solid phase species and temperature coupled with the heterogeneous reactions and the interphase transport (eqs. (34)-(35)). To do so, an ODE solver can be adopted to treat the stiffness and non-linearity of the heterogeneous reactions as successfully used in the literature [64].
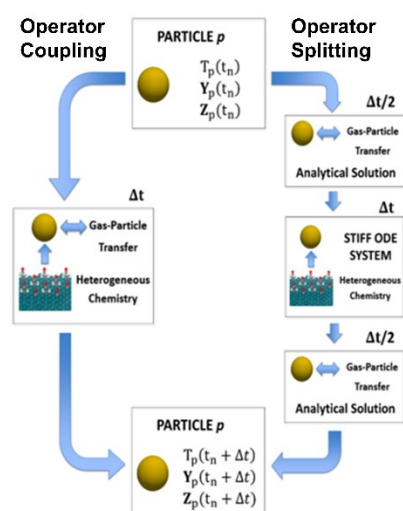

Figure 4. Schematic representation of the Operator Splitting (right branch) and the Operator Coupling (left branch) numerical strategies. Adapted with permission from ref. [63].

This numerical strategy can be exploited also in the context of a Eulerian-Eulerian description of the multiphase flow. However, the segregated resolution of the two phases usually introduces numerical errors when long time steps (i.e., above 5e^{-6} s) are used. Consequently, the resolution of the reactivity by means of the OC can limit the performances of the Euler-Euler model approach hindering the solution of detailed chemical kinetics along with the whole dynamic of pilot or industrial units [77].

2.2.4.4 Operator Splitting Method

Coherently with the fixed bed reactor, also the OS approach can be applied to solve the governing equations of fluidized systems both in the context of Euler-Lagrange [63,64] and Euler-Euler models.
As for the OC, the OS involves the complete segregation of the fluid and the solid phase, and thus this limits the performances of the Euler-Euler model to treat pilot or industrial units. In the context of the Eulerian-Lagrangian description of the multiphase flow, the OS can be efficiently applied since the segregated solution of the two phases is mandatory. In this view, the OS, schematized in the right branch of **Figure 4**, decouples the reactive terms (R_j^{het}, Q^{het}) from the species and energy balance equations and solves them in three sequential steps (Strang approach [52]). First, the thermo-chemical composition is updated by solving only the transport equation (eq. (42)- (43)) over one half of the simulation time step by means of a linear matricial solver.

$$V_p \frac{d(\rho_{f,p}\kappa_s\omega_{j,p})}{dt} = -Kc_jA_p\bar{\rho}(\omega_{j,p} - \omega_{j,f}) \tag{42}$$

$$(1 - \kappa_s)\rho_p c_{p,p} V_p \frac{dT_p}{dt} = -hA_p(T_p - T_f) \tag{43}$$

Then, the equations accounting for the reactive terms (eqs. (44)-(45)) are solved over the entire time step by adopting an ODE solver able to treat the stiffness and non-linearity related to the chemical reaction rates.

$$V_p \frac{d(\rho_{f,p}\kappa_s\omega_{j,p})}{dt} = V_p R_j^{het} \tag{44}$$

$$(1 - \kappa_s)\rho_p c_{p,p} V_p \frac{dT_p}{dt} = V_p Q^{het} \tag{45}$$

Finally, the last update of the species is carried out by solving the transport equations over half time step, similarly to the first step.
This strategy has been successfully applied to simulate lab-scale bubbling beds [63] by adopting a microkinetic scheme describing the catalytic partial oxidation of methane [82,83] and it provides a 2-fold reduction of the computational cost with respect to the OC.
However, this numerical strategy needs an accurate selection of the simulation time step. Indeed, in order to avoid numerical deviations, the simulation time step must be properly set lower than the characteristic time of the phenomena [64]. Consequently, this condition requires a reduction of the simulation time step usually adopted in literature (e.g., 5e^{-6} s) if species with a high diffusivity (e.g., hydrogen) are present in the system, with consequent increment of the computational effort of the strategy [64].

3 Speed-up Strategies

The multiscale description of the chemistry inside the reactor units by means of the previously described modeling approaches requires a significant computational cost which has been estimated in around 70-90% of the overall simulation time [84]. Consequently, speed-up methodologies have been developed in the literature to improve the performances of these strategies by reducing the cost related to the detailed surface reactivity. In particular, the different strategies can be divided into two distinct approaches: on-the-fly and pre-computation of the chemical kinetics approaches.

3.1 On-the-fly Strategies

According to the on-the-fly strategies, the chemistry is solved during the simulation and the reduction of the computational cost is achieved by diminishing the number of computationally-intensive ODE evaluations of the surface chemistry source terms. This reduction can be achieved by exploiting the results of prior integrations or by considering the similarities between the systems that must be solved.

3.1.1 In Situ Adaptive Tabulation

The In Situ Adaptive Tabulation (ISAT), developed by Pope [85], is a storage and retrieval strategy aimed at reducing computationally expensive calculations in dynamic simulations. In doing so, during the simulation, the ISAT algorithm tabulates the results obtained by the computational demanding ODE integrations in order to replace the next ones with an efficient and accurate approximation by the stored value. The storage structure is a binary tree that is composed of 2 elements, the nodes, which allow the research in the binary tree, and the leaves, which contain all the information needed to approximate the integration outcomes. The binary tree is empty at the beginning of the simulations and the leaves are added based on the integrations performed by the ODE solver. The information stored in a leaf consists of the initial conditions, the integration outcomes, a mapping gradient, that is used to perform the linear approximation of the outcomes, and a region of accuracy. This region is defined as the connected region containing all the initial conditions providing a local error below a specified tolerance and it is approximated with an ellipsoid of accuracy (EOA). The strategy can perform three different actions: retrieve, grow and add. Given an initial condition, several search strategies are performed to find the EOA of a certain leaf that contains that initial condition. If the EOA is found, the "retrieve" action occurs and the outcome is evaluated as a linear approximation of the stored solution. Conversely, the solution of the system is obtained by means of the direct ODE integration. The approach then verifies whether it is possible to enlarge the EOA of a selected leaf that is close to the initial condition employed for the integration (growth attempt). To do so, the solution obtained by direct ODE integration is compared with the linear approximation of the outcomes stored in the selected leaf. If the deviation is less than the specified tolerance, the "grow" action occurs and the EOA of the selected leaf is grown to also cover the new initial conditions. In contrast, the "add" action occurs and a new leaf is added to the binary tree.

In addition, its application in transient problems requires the introduction of a cleaning procedure inside the ISAT algorithm. Indeed, the chemical evolution of the system is linked to a very broad range of compositions. During the simulation, a certain composition could not be any more present in the reactor environment, and thus, its presence in the binary tree becomes useless and decrease the efficiency of the strategy. Consequently, the cleaning procedure aims at removing the leaves of the binary tree characterized by a composition that cannot be obtained anymore in the reactor environment.

The ISAT approach has been efficiently exploited to reduce the computational cost of the reaction step of the OS both in fixed bed and fluidized reactors. In fixed bed units, it has been able to provide a 15-fold reduction of the whole computational cost in a packed bed composed of 25 spheres (about 96,000 reactive cells) [84] by adopting a microkinetic scheme for the methane steam reforming process [82]. In fluidized systems, a 4-fold reduction of the computational cost has been achieved in a lab-scale fluidized bed reactor composed of 10000 catalytic particles [63] whose reactivity is described by means of a microkinetic scheme for the methane catalytic partial oxidation process [82,83]. However, the ISAT strategy cannot be applied to steady-state solvers [84].

3.1.2 Agglomeration Approaches

In addition to the ISAT, a technique based on cell agglomeration [86] has been proposed to treat detailed heterogeneous chemistries both in transient and steady-state simulations [18,64]. This approach aims at reducing the number of integrations required in a time step or iteration by grouping the computational cells having similar operating conditions in bins, as schematized in **Figure 5** (a). In doing so, the number of

integrations required to solve the system is reduced becoming equal to the number of the bins. Then, the resulting composition is mapped back to the cells.

This strategy has been successfully applied to multi-region simulations of fixed bed reactors. Indeed, it enabled a simulation of a packed bed composed of 66 spherical particles (about 0.6 M reactive cells) [18] operated with a detailed microkinetic description of the catalytic partial oxidation of methane [82,83] with a 14-fold reduction of the computational cost.

(a)   (b)
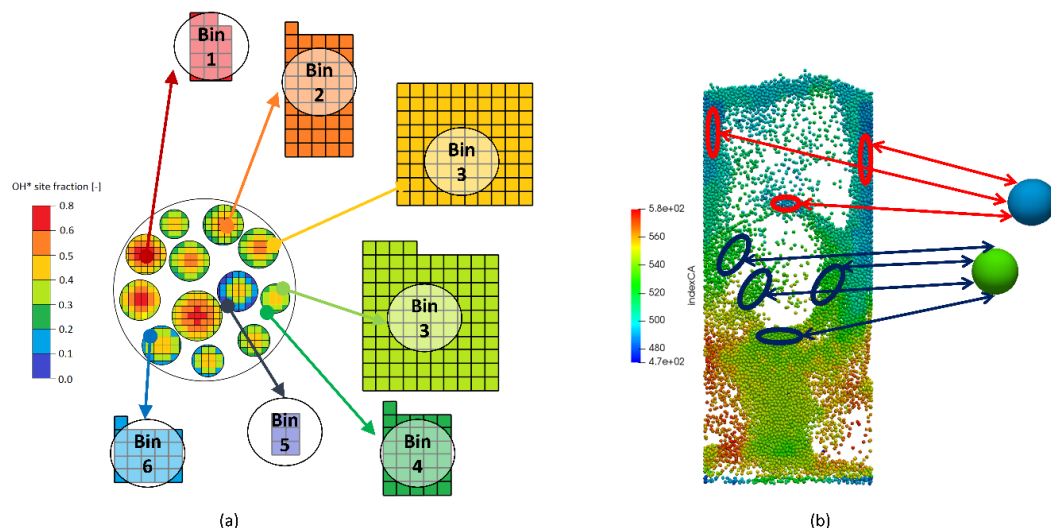
Figure 5. Schematic representation of the agglomeration approach adopted in the steady-state simulation of fixed bed reactors (a) and in OC simulations of lab-scale fluidized units (b). Adapted with permission from ref. [64].

Then, this speed-up strategy has been extended to treat also dynamic simulations of Euler-Lagrange description of fluidized reactors by means of the Operator Coupling approach [64]. In this application, the agglomeration algorithm is used to group in bins particles with similar initial conditions (**Figure 5** (b)), in order to reduce the number of particles that have to be integrated in a time step. By doing so, this strategy has provided a 6-fold reduction of the computational cost in a lab-scale fluidized reactor with 10^4 catalytic particles [64] operated with a kinetic description of the CO methanation process [87]. Then, it has allowed for the simulation of a lab-scale fluidized unit composed of 1.2 million reactive particles [64].

3.2 Pre-computation of the Chemical Kinetics

In addition to the on-the-fly strategies, the reduction of the computational effort of the multiscale CFD approaches can be achieved by pre-computing and tabulating the chemical kinetic [88]. In literature, this strategy is mainly used for kinetics characterized by a computationally demanding calculation of the rates (i.e., high dimension mean-field kinetics, kMC) [89]. This approach requires the computation of a dataset beforehand the beginning of the simulation that must be properly tabulated in order to be efficiently used during the simulation. In this view, a proper tabulation technique and data generation strategy must be selected to efficiently and accurately apply this strategy.

Concerning the tabulation technique, it is necessary to move from a discrete information of the pre-computed data to a continuous one. The tabulation algorithm assumes a crucial role since it affects the computational efficiency and accuracy of the numerical strategy and consequently, different approaches have been proposed in the literature. The simplest one consists of the approximation of the function by adopting multidimensional splines [90–95]. Accordingly, a polynomial-like expression is exploited to describe the target function. However, their application to functions characterized by abrupt changes in catalytic activity is challenging [88]. To overcome such a limitation, a more complex method (e.g., Shepard interpolation) has been proposed to improve the prediction of the spline approach. It revealed to provide an excellent approximation of the complex reaction rates which characterize kMC simulations [88,96,97]. However, the accuracy and efficiency of these two approaches are strongly dependent on the size of the

kinetic scheme, and thus their applicability for complex kinetic schemes is hampered [89,93]. In literature, the problem related to the efficient treatment of high size datasets both in terms of variables and records has been solved by adopting Machine Learning approaches [98]. Thus, these approaches have been recently proposed to efficiently tabulate high dimension schemes [99].

Concerning the data generation, in literature different approaches are present. The simplest approach, usually adopted in the context of mean fields models [90,99], consists of evenly distributed or randomly located points in each direction of the space. Nonetheless, since no information on the function is considered, a large dataset (e.g., hundreds of thousands of records) is often required to achieve an accurate prediction. When the generation of these records is computationally demanding (e.g., in the case of kMC calculations), this approach requires a very high computational effort to build-up the dataset [93,94] which reduces the overall efficiency of the method. In this respect, the definition of the training set becomes key to achieve high accuracy with a concomitant reduction of the computational effort. To this aim, a dedicated numerical strategy has been proposed to minimize the number of data points needed to achieve a target level of accuracy [89] (**Figure 6**).
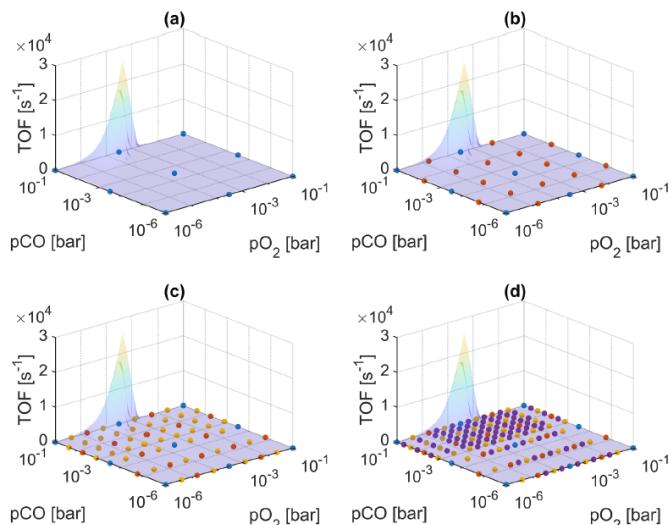

Figure 6. Evolution of the dataset adopted in the iterative procedure by means of Random Forest from the first iteration (a) to the last one (d). Adapted with permission from ref. [89].

To do so, an adaptive procedure able to selectively add points only in the region of the space where the approximation of the function is more challenging has been proposed. Accordingly, few points in each direction of the space defined by the relevant variables are firstly considered (**Figure 6** (a)). Then, the importance of each variable is evaluated by taking advantage of the Machine learning features. In doing so, it is possible to select for the refinement of the dataset just the variables which mostly influence the function. Then, the algorithm adds new points only in the space region where the function shows sharp variation of its value (**Figure 6** (b)-(c)). Therefore, this approach can minimize the dimension of the dataset required to reach a certain accuracy (**Figure 6** (d)) and thus the computational effort.

The pre-computation of the chemical kinetics has been successfully adopted to simulate a fixed bed reactor [99] with a complex microkinetic scheme describing ethylene oxidation [100]. In addition, this approach has been efficiently used to simulate a structured fixed bed with a complex kMC description of the CO oxidation on RuO_2(110) [89], becoming the enabling factor to treat chemistries characterized by a very computational demanding calculation of the rates.

However, it could be exploited also to substitute the computationally demanding on-the-fly ODE integrations by pre-computing and tabulating their outcomes.

4   Hierarchical approach to Chemical Reaction Engineering

The CFD multiscale modeling approaches are crucial for the fundamental investigation of the phenomena occurring in a catalytic units. However, their computational effort limits the applicability of such

approaches, and thus, they are not suitable for routinely analysis and design of the entire catalytic reactor (i.e., model predictive control) [101]. Macroscopic 1D or 2D reactor models are required for this purpose. Typically, these models are based on empirical parameters and engineering correlations usually obtained by means of experimental investigations . The accuracy and reliability of the macroscopic reactor models roots on the quality of the lumped parameters employed for the description of the transport properties. In case of conventional reactors and catalytic supports, these parameters may be available for some specific geometries and range of operative conditions. Hence, their validity is confined to conditions where they have been derived. The situation is even more complex for new designs for which is unlikely to have precise engineering correlations and lumped parameters. To overcome such problems, a hierarchical approach [30,102], sketched in **Figure 7**, has been proposed to replace the empirical nature of the lumped parameters with the information extracted by the detailed analysis of the system, based on first-principles multiscale investigations of the catalytic environment.
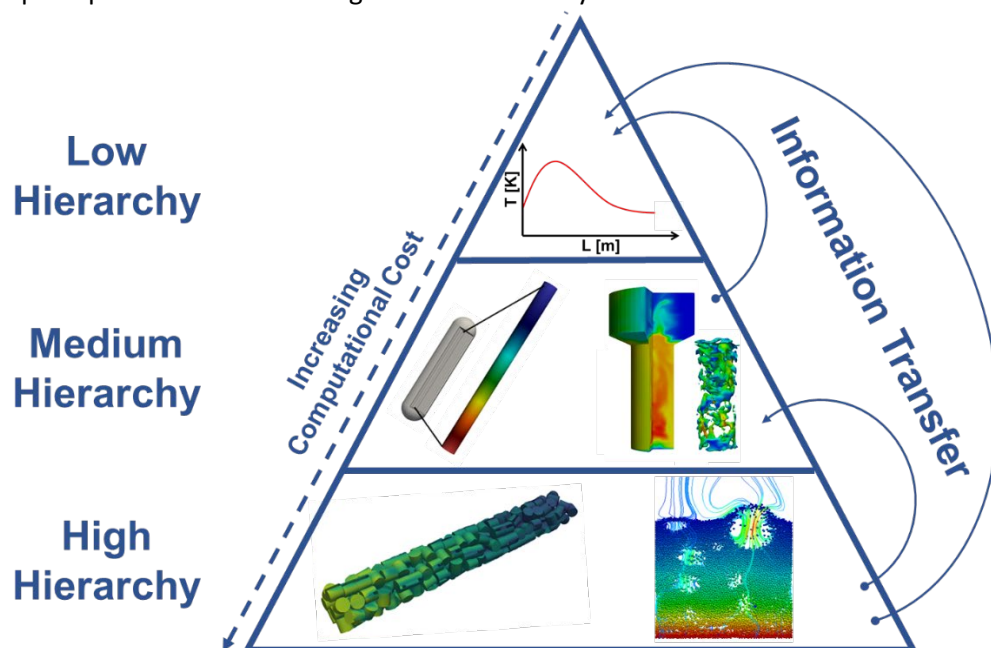

Figure 7. Schematic representation of the hierarchical approach.

According to the hierarchical approach, the detailed simulations of selected number of geometries and operating conditions focused on a specific aspect of the full problem (e.g. mass transport, pressure drop) is considered on a limited portion of the entire system which is still representative of the phenomena under investigation. Based on the CFD results, suitable correlations accounting for the multiscale nature of the catalytic environment [15,30,31,102] were developed and adopted to improve the accuracy of the macroscopic reactor model (low hierarchy). This approach was successfully applied in the field of fixed bed reactors to investigate novel reactor configurations (e.g., micro-channel reactors, Open Cell Foam) for which macroscopic models were still not available. In particular, it was proven that the correlations developed for micro-channel reactors allow for their investigation through lumped models with only small deviations with respect to the detailed approach ones [30,102]. On top of this, the engineering correlations derived from the hierarchical approach can also be employed in CFD-based porous media models of fixed bed reactors (medium hierarchy). In doing so, it is possible to investigate reactor geometries whose description with conventional macroscopic models requires the adoption of too simplifying hypothesis with a reasonable computational cost.

The hierarchical approach can be extended also in the context of fluidized units. Also here, the computational effort of the high hierarchy approach to describe fluidized systems (i.e., Euler-Lagrange) limits its application to lab-scale units. Hence, the description of pilot or industrial units requires the adoption of a Eulerian-Eulerian description or the multiphase flow (medium hierarchy) or macroscopic reactor models (low hierarchy). In both cases, these modeling approaches are based on closure models

for the description of the unresolved scales and thus the hierarchical approach can be employed to derive engineering parameters aiming at improving the description of these systems by employing the information gained at the highest resolution into lower hierarchy methods.

5   Conclusions and Future Perspectives

This work deals with the critical discussion of the multiscale modeling approaches to fundamentally investigate heterogeneous catalytic reactors, primarily focusing on the combination between CFD modeling approaches and first-principles chemical kinetic. The inherent complexity and wide variety of the typical catalytic systems require the development of several methods and strategies to tackle challenges related to the treatment of the stiff and non-linear reaction source terms. In this view, the chemical reactors have been subdivided in two different categories, i.e., fixed bed and fluidized, and different strategies have been reviewed with respect to their ability to describe the characteristic phenomena in the reactor configurations. Nonetheless, the main issue related to the usage of these strategies is still the computational effort needed to solve the detailed chemical kinetics, as it results in the 70-90% of the overall computational cost. To tackle this problem, different speed-up strategies (i.e., on-the-fly and pre-computation of the chemical kinetics) have been developed to reduce the computational burden of the evaluation of the detailed chemical kinetics. Finally, the hierarchical approach, which aims at the improvement of the accuracy of the lumped models for reactor analysis and design, was discussed.

Despite the successful developments reviewed in this paper, different topics are still under investigation in the context of the reactive multiscale modeling:

1.   Deeper understanding of the intra-particle phenomena: this topic involves questions related to how a detailed description of the catalyst porous matrix can be included in the multiscale modeling approach. Hence, scientific research on this topic should provide fundamental insights regarding the species and heat transport inside the catalyst porous structures and their relation with the internal catalyst properties (e.g., porosity, tortuosity, pore size distribution).

2.   Combination of multiscale modeling with innovative computational methods: the computational effort related to the multiscale description of catalytic systems hinders the modeling of large and challenging systems. In this view, the application of innovative numerical methods (e.g., machine learning) in the context of chemical reaction engineering could overcome these limitations to provide accurate predictions with an affordable computational effort.

3.   Extension of the multiscale approach to gas-solid-liquid catalytic systems [103]: scientific research on this topic should aim at improving the reactive multiscale modeling approach to account for the presence of more than two phases inside the catalytic environment. It should allow for the fundamental investigation of relevant applications (e.g., trickle bed or slurry reactors), whose performances are strongly related to the interactions between the three phases.

4.   Application of the hierarchical approach to chemical reaction engineering: a larger utilization of the hierarchical modeling approach both in the context of fixed and fluidized units should allow for the formulation of engineering correlations accounting for the multiscale nature of the catalytic environment. As such, medium or low hierarchy models could be improved to provide still accurate predictions but with a reduced computational effort with respect to the high hierarchy ones.

Picture and Short CV

Daniele Micale graduated with full marks in Chemical Engineering earing the Master degree at the Politecnico di Milano (Italy) in 2019. His Master Thesis work, performed in the Laboratory of Catalysis and Catalytic Processes under the supervision of Prof. Matteo Maestri, consisted in the investigation of speed-up strategies for the multiscale simulations of fluidized systems. Since November 2019, he is Ph.D. Student at Politecnico di Milano in the group of Prof. Matteo Maestri which is active in the field of the CFD Multiscale Modeling of Heterogeneous Catalytic reactors (e.g. ERC SHAPE and H2020 ReaxPro projects). His main research topics focus on the development of multiscale methodologies for the description of industrial fluidized units. In particular, these methodologies are applied in the ARPA-E project led by Prof. Matteo Pasquali in collaboration with Prof. Matteo Maestri whose target is the industrial synthesis of carbon nanotubes with a positive turquoise hydrogen output.

Claudio Ferroni graduated in Chemical Engineering earning the Master Degree at the Politecnico di Milano (Italy) in 2019. His Master Thesis work, performed in the Laboratory of Catalysis and Catalytic Processes under the supervision of Prof. Enrico Tronconi, Prof. Gianpiero Groppi and Prof. Matteo Maestri, consisted in the fundamental investigation of the transport properties of structured support for catalytic applications by means of Computational Fluid Dynamic. Since November 2019 he is PhD Student at Politecnico di Milano in the group of Prof. Enrico Tronconi, Prof. Gianpiero Groppi and Prof. Matteo Maestri. His main research activity consists of the multiscale modelling of fixed bed reactors. In particular, his work is devoted to the fundamental investigation of transport properties in innovative structured materials as enhanced supports for catalytic applications.

Riccardo Uglietti graduated with full marks in Chemical Engineering earing the Master degree at the Politecnico di Milano (Italy) in 2017. He performed his Master Thesis in the Laboratory of Catalysis and Catalytic Processes under the supervision of Prof. Matteo Maestri, developing a CFD multi-scale model for catalytic fluidized systems. Since November 2017, he is Ph.D. Student at Politecnico di Milano in the group of Prof. Matteo Maestri which is active in the field of the CFD Multiscale Modeling of Heterogeneous Catalytic reactors (e.g. ERC SHAPE and H2020 ReaxPro projects). His main research topics focus on the development of reactive CFD methodologies including the microkinetic description of catalytic reactions in both lab and industrial fluidized bed reactors. During his Ph.D., he spent 7 months joining the group of Prof. J.R. van Ommen, as a visiting researcher at the Delft University of Technology (NL), for the experimental investigation of lab scale fluidized beds.

Mauro Bracconi is an Assistant Professor of Chemical Engineering at the Laboratory of Catalysis and Catalytic Processes, Politecnico di Milano, Italy. He received the Ph.D. in Chemical Engineer at the Politecnico di Milano in 2018. He has been visiting scholar at the School of Chemical Engineering & Analytical Science, University of Manchester (UK) from February 2017 to July 2017 and at the Delaware Energy Institute of University of Delaware (USA) in June 2019. His main research interests are in the field of multiscale modeling of heterogeneous catalytic processes using Computational Fluid Dynamics and the investigation of transport phenomena in

structured supports for process intensification. His interests also regard the development of numerical methodologies to couple first-principles kinetics in detailed fluid dynamic simulations using machine learning and artificial intelligence methods.

Matteo Maestri is a full professor of Chemical Engineering at Politecnico di Milano, Italy. He received his Ph.D. in Chemical Engineering from Politecnico di Milano in 2008. He was a visiting scholar at the Center for Catalytic Science and Technology of the Department of Chemical Engineering of the University of Delaware, USA (2006–2007); Alexander von Humboldt Fellow at the Fritz-Haber-Institut der Max-Planck-Gesellschaft in Berlin, Germany (2009–2010); and at the Catalysis Research Center (CRC)–Department of Chemistry of the Technische Universität München, Germany (2011). He has received several awards, including the ERC Starting Grant from the European Research Council. In 2021, he has been named "TUM Ambassador" by the Technische Universität München, Germany. He is the head of the research group on multiscale analysis of chemical catalytic processes at the Laboratory of Catalysis and Catalytic Processes. His main research interests are fundamental analysis of catalytic kinetics and multiscale modeling of catalytic processes, by applying and developing methods that span from atomistic (DFT) calculations to CFD, and from kinetic analysis to operando-spectroscopy.

Symbols used

A	Geometrical area
c_p	Heat capacity at constant pressure
$\bar{c}_p$	Average heat capacity at constant pressure
$\hat{c}_p$	Mean local heat capacity at constant pressure
$\mathfrak{D}$	Mixture average diffusion coefficient
$\boldsymbol{F}$	Force vector
$\boldsymbol{g}$	Gravity vector
h	Heat transfer coefficient
$\boldsymbol{I}$	Identity matrix
$\boldsymbol{J}$	Diffusion flux
Kc	Mass transfer coefficient
L_{char}	Characteristic length
m	Mass
M	Vector of rate change of a generic variable due to transport process
Nu	Nusselt number
p	Pressure
$\hat{p}$	Mean local pressure
$\boldsymbol{q}_{cond}$	Conduction heat flux
Q	Heat released by the reactions
R	Production rate
S	Vector of rate change of a generic variable due to chemical reactions
Sh	Sherwood number
S_v	Specific surface area
$S\omega$	Fluid-solid mass transfer
t	Time
T	Temperature
$\hat{T}$	Mean local temperature
$\boldsymbol{U}$	Velocity vector
V	Volume

Greek letters

∇	Gradient
ε	Void fraction
θ	Adsorbed species site fraction
$\hat{\theta}$	Mean local adsorbed species site fraction
κ	Porosity
λ	Thermal conductivity
$\hat{\lambda}$	Mean local thermal conductivity
μ	Viscosity
$\hat{\mu}$	Mean local viscosity
Π	Source term accounting for the pressure drop in the porous medium
ρ	Density
$\bar{\rho}$	Average density between the fluid and the solid phase
$\hat{\rho}$	Mean local density
σ_{cat}	Concentration of the active sites on the catalyst surface
$\bar{\bar{\tau}}$	Stress tensor
φ	Generic Variable
Ψ	Fluid-solid heat transfer
ω	Species mass fraction
$\hat{\omega}$	Mean local species mass fraction

Sub- and Superscrits

0	Initial conditions
b	Buoyancy
cat	Catalyst
$coll$	Collisions
d	Drag
eff	Effective
f	Fluid phase
$f \rightarrow s$	Fluid to solid
het	Heterogeneous reactions
hom	Homogeneous reactions
I	Interface
j	Index of the gas-phase species
k	Index of the adsorbed species
p	Index of the particles
s	Solid phase
T	Transpose

Abbreviations

CAD	Computer-Aided Design
CFD	Computational Fluid Dynamic
DEM	Discrete Element Method
DNS	Direct Numerical Simulations
EOA	Ellipsoid of Accuracy
ISAT	In Situ Adaptive Tabulation
kMC	Kinetic Monte Carlo
KTGF	Kinetic Theory of Granular Flow
LRS	Linearization of the Reaction Source term
MOS	Multiphase Operator Splitting
OC	Operator Coupling
OCM	Oxidative Coupling of Methane

ODE	Ordinary Differential Equations
OS	Operator Splitting
PDE	Partial Differential Equations
POCS	Periodic Open Cellular Structures
REV	Representative Elementary Volume
RSBC	Reaction Source Terms as Boundary Condition
VAT	Volume Averaging Technique

References

[1]   M. I. Alam, R. Cheula, G. Moroni, L. Nardi, M. Maestri, *Catal. Sci. Technol.* **2021**, *11* (20), 6601–6629. DOI: 10.1039/d1cy00922b.

[2]   M. Maestri, *Chem. Commun.* **2017**, *53* (74), 10244–10254. DOI: 10.1039/c7cc05740g.

[3]   M. P. Dudukovic, *Science (80-.).* **2009**, *325* (5941), 698–701. DOI: 10.1126/science.1174274.

[4]   A. Bruix, J. T. Margraf, M. Andersen, K. Reuter, *Nat. Catal.* **2019**, *2* (8), 659–670. DOI: 10.1038/s41929-019-0298-3.

[5]   M. Maestri, in *Annu. Meet. Ger. Subj. Gr. Chem. React. Eng.*, Würzburg, Germany **2021**.

[6]   M. Maestri, A. Cuoci, *Chem. Eng. Sci.* **2013**, *96*, 106–117. DOI: 10.1016/j.ces.2013.03.048.

[7]   A. L. Tonkovich, E. Daymo, Springer International Publishing, Cham **2018**.

[8]   P. Forzatti, I. Nova, E. Tronconi, *Angew. Chemie*. **2009**, *121* (44), 8516–8518. DOI: 10.1002/ange.200903857.

[9]   E. Tronconi, G. Groppi, C. G. Visconti, *Curr. Opin. Chem. Eng.* **2014**, *5*, 55–67. DOI: https://doi.org/10.1016/j.coche.2014.04.003.

[10]   N. Jurtz, M. Kraume, G. D. Wehinger, *Rev. Chem. Eng.* **2019**, *35* (2), 139–190. DOI: 10.1515/revce-2017-0059.

[11]   A. G. Dixon, M. Nijemeisland, E. H. Stitt, *Adv. Chem. Eng.* **2006**, *31* (06), 307–389. DOI: 10.1016/S0065-2377(06)31005-8.

[12]   M. Quintard, S. Whitaker, *Transp. Porous Media*. **1994**, *14* (2), 179–206. DOI: 10.1007/BF00615200.

[13]   S. Whitaker, *Ind. Eng. Chem.* **1969**, *61* (12), 14–28.

[14]   M. Bracconi, M. Ambrosetti, M. Maestri, G. Groppi, E. Tronconi, *Chem. Eng. J.* **2017**, *315*, 608–620. DOI: 10.1016/j.cej.2017.01.069.

[15]   C. Ferroni, M. Bracconi, M. Ambrosetti, M. Maestri, G. Groppi, E. Tronconi, *Ind. Eng. Chem. Res.* **2021**, *60* (29), 10522–10538. DOI: 10.1021/acs.iecr.1c00215.

[16]   O. S. P. Cundall, *Geotechnique*. **1979**, *29* (1), 47–65. DOI: 10.1016/0148-9062(79)91211-7.

[17]   A. G. Dixon, G. Walls, H. Stanness, M. Nijemeisland, E. H. Stitt, *Chem. Eng. J.* **2012**, *200–202*, 344–356. DOI: 10.1016/j.cej.2012.06.065.

[18]   S. Rebughini, A. Cuoci, A. G. Dixon, M. Maestri, *Comput. Chem. Eng.* **2017**, *97*, 175–182. DOI: 10.1016/j.compchemeng.2016.11.033.

[19]   M. Ambrosetti, M. Bracconi, M. Maestri, G. Groppi, E. Tronconi, *Chem. Eng. J.* **2020**, *382* (September 2019), 1–6. DOI: 10.1016/j.cej.2019.122801.

[20]   G. Boccardo, F. Augier, Y. Haroun, D. Ferré, D. L. Marchisio, *Chem. Eng. J.* **2015**, *279*, 809-820–820. DOI: 10.1016/j.cej.2015.05.032.

[21]   V. Papetti, P. Dimopoulos Eggenschwiler, A. Della Torre, F. Lucci, A. Ortona, G. Montenegro, *Int. J. Heat Mass Transf.* **2018**, *126*, 1035–1047. DOI: 10.1016/j.ijheatmasstransfer.2018.06.061.

[22]   F. Lucci, A. Della Torre, G. Montenegro, R. Kaufmann, P. Dimopoulos Eggenschwiler, *Int. J. Heat Mass Transf.* **2017**, *108*, 341–350. DOI: 10.1016/j.ijheatmasstransfer.2016.11.073.

[23]   M. Sun, M. Li, C. Hu, L. Yang, Y. Song, D. Tang, J. Zhao, *Appl. Therm. Eng.* **2021**, *182* (July 2020), 116130. DOI: 10.1016/j.applthermaleng.2020.116130.

[24]   G. D. Wehinger, H. Heitmann, M. Kraume, *Chem. Eng. J.* **2016**, *284*, 543–556. DOI: 10.1016/j.cej.2015.09.014.

[25]   S. Rebughini, A. Cuoci, M. Maestri, *Chem. Eng. Sci.* **2016**, *141*, 240–249. DOI: 10.1016/j.ces.2015.11.013.

[26] A. G. Dixon, M. Nijemeisland, E. H. Stitt, *Comput. Chem. Eng.* **2013**, *48*, 135–153. DOI: 10.1016/j.compchemeng.2012.08.011.

[27] D. Rong, M. Horio, *2nd Int. Conf. CFD Miner. Process Ind.* **1999**, (December), 65–70.

[28] G. D. Wehinger, C. Füterer, M. Kraume, *Ind. Eng. Chem. Res.* **2017**, *56* (1), 87–99. DOI: 10.1021/acs.iecr.6b03596.

[29] M. Kutscherauer, S. Böcklein, G. Mestl, T. Turek, G. D. Wehinger, *Chem. Eng. J. Adv.* **2022**, *9*, 100197. DOI: https://doi.org/10.1016/j.ceja.2021.100197.

[30] S. Rebughini, A. Cuoci, M. Maestri, *Chem. Eng. J.* **2016**, *289*, 471–478. DOI: 10.1016/j.cej.2015.12.089.

[31] M. Bracconi, M. Ambrosetti, M. Maestri, G. Groppi, E. Tronconi, *Chem. Eng. J.* **2018**, *352* (February), 558–571. DOI: 10.1016/j.cej.2018.07.023.

[32] R. B. Bird, W. E. Stewart, E. N. Lightfoot, *Transport Phenomena*, 2nd ed. **2007**.

[33] H. Karadeniz, C. Karakaya, S. Tischer, O. Deutschmann, *Chem. Eng. Sci.* **2013**, *104*, 899–907. DOI: https://doi.org/10.1016/j.ces.2013.09.038.

[34] H. Karadeniz, C. Karakaya, S. Tischer, O. Deutschmann, *Zeitschrift für Phys. Chemie*. **2015**, *229* (5), 709–737. DOI: doi:10.1515/zpch-2014-0622.

[35] G. D. Wehinger, F. Klippel, M. Kraume, *Comput. Chem. Eng.* **2017**, *101*, 11–22. DOI: https://doi.org/10.1016/j.compchemeng.2017.02.029.

[36] R. E. Hayes, P. K. Mok, J. Mmbaga, M. Votsmeier, *Chem. Eng. Sci.* **2007**, *62* (8), 2209–2215. DOI: https://doi.org/10.1016/j.ces.2007.01.018.

[37] T. Maffei, G. Gentile, S. Rebughini, M. Bracconi, F. Manelli, S. Lipp, A. Cuoci, M. Maestri, *Chem. Eng. J.* **2016**, *283*, 1392–1404. DOI: 10.1016/j.cej.2015.08.080.

[38] B. Partopour, A. G. Dixon, *ChemEngineering* . **2018**, *2* (1). DOI: 10.3390/chemengineering2010002.

[39] P. Kočí, F. Štěpánek, M. Kubíček, M. Marek, *Chem. Eng. Sci.* **2006**, *61* (10), 3240–3249. DOI: https://doi.org/10.1016/j.ces.2005.12.008.

[40] A. Della Torre, G. Montenegro, A. Onorati, T. Cerri, E. Tronconi, I. Nova, in *SAE 2020 World Congr. Exp. WCX 2020*, Vol. 2020, SAE International **2020**.

[41] S. Meinicke, K. Dubil, T. Wetzel, B. Dietrich, *Int. J. Heat Mass Transf.* **2020**, *149*, 119201.

[42] R. K. Shah, A. L. London, *Laminar Flow Forced Convection in Ducts: A Source Book for Compact Heat Exchanger Analytical Data*, Academic Press **2014**.

[43] S. Ergun, A. A. Orning, *Ind. Eng. Chem.* **1949**, *41* (6), 1179–1184.

[44] I. F. Macdonald, M. S. El-Sayed, K. Mow, F. A. L. Dullien, *Ind. Eng. Chem. Fundam.* **1979**, *18* (3), 199–208. DOI: 10.1021/i160071a001.

[45] M. Bracconi, M. Ambrosetti, O. Okafor, V. Sans, X. Zhang, X. Ou, C. P. Da Fonte, X. Fan, M. Maestri, G. Groppi, et al., *Chem. Eng. J.* **2019**, *377*, 120123. DOI: https://doi.org/10.1016/j.cej.2018.10.060.

[46] N. Wakao, S. Kagei, *Heat and Mass Transfer in Packed Beds*, Vol. 1, Taylor & Francis **1982**.

[47] R. Cònsul, C. D. Pérez-segarra, K. Claramunt, J. Cadafalch, A. Oliva, *Combust. Theory Model.* **2003**, *7* (3), 525–544. DOI: 10.1088/1364-7830/7/3/305.

[48] M. D. Smooke, R. E. Mitchell, D. E. Keyes, *Combust. Sci. Technol.* **1986**, *67* (4–6), 85–122. DOI: 10.1080/00102208908924063.

[49] Z. Ren, S. B. Pope, *J. Comput. Phys.* **2008**, *227* (17), 8165–8176. DOI: 10.1016/j.jcp.2008.05.019.

[50] M. S. Day, J. B. Bell, *Combust. Theory Model.* **2000**, *4* (4), 535–556. DOI: 10.1088/1364-7830/4/4/309.

[51] J. Kim, S. Y. Cho, *Atmos. Environ.* **1997**, *31* (15), 2215–2224. DOI: https://doi.org/10.1016/S1352-2310(97)88636-0.

[52] G. Strang, *SIAM J. Numer. Anal.* **1968**, *5* (3), 506–517. DOI: 10.1137/0705041.

[53] M. Maestri, A. Beretta, T. Faravelli, G. Groppi, E. Tronconi, D. G. Vlachos, *Chem. Eng. Sci.* **2008**, *63* (10), 2657–2669. DOI: https://doi.org/10.1016/j.ces.2008.02.024.

[54] A. G. Dixon, M. E. Taskin, M. Nijemeisland, E. H. Stitt, *Ind. Eng. Chem. Res.* **2010**, *49* (19), 9012–9025. DOI: 10.1021/ie100298q.

[55] D. Kunii, O. Levenspiel, *Fluidization Engineering* **1991**.

[56] N. G. Deen, E. A. J. F. Peters, J. T. Padding, J. A. M. Kuipers, *Chem. Eng. Sci.* **2014**, *116*, 710–724. DOI: 10.1016/j.ces.2014.05.039.

[57] N. G. Deen, M. Van Sint Annaland, M. A. Van der Hoef, J. A. M. Kuipers, *Chem. Eng. Sci.* **2007**, *62*

(1–2), 28–44. DOI: 10.1016/j.ces.2006.08.014.

[58]   Y. Tsuji, T. Tanaka, T. Ishida, *Powder Technol.* **1992**, *71*, 239–250. DOI: 10.1016/0032-5910(92)88030-L.

[59]   B. P. B. Hoomans, J. A. M. Kuipers, W. J. Briels, W. P. M. Van Swaaij, *Science (80-.).* **1996**, *51* (1), 99–118. DOI: 10.1016/0009-2509(95)00271-5.

[60]   D. Gidaspow, *Multiphase Flow and Fluidization: Continuum and Kinetic Theory Descriptions*, Academic Press **1994**.

[61]   Y. Liu, O. Hinrichsen, *Ind. Eng. Chem. Res.* **2014**, *53* (22), 9348–9356. DOI: 10.1021/ie500774s.

[62]   Z. Peng, E. Doroodchi, C. Luo, B. Moghtaderi, *AIChE J.* **2014**, *60* (6), 2000–2018. DOI: https://doi.org/10.1002/aic.14421.

[63]   R. Uglietti, M. Bracconi, M. Maestri, *React. Chem. Eng.* **2018**, *3* (4), 527–539. DOI: 10.1039/c8re00050f.

[64]   R. Uglietti, M. Bracconi, M. Maestri, *React. Chem. Eng.* **2020**, *5* (2), 278–288. DOI: 10.1039/c9re00440h.

[65]   H. Zhou, G. Flamant, D. Gauthier, *Chem. Eng. Sci.* **2004**, *59* (20), 4205–4215. DOI: https://doi.org/10.1016/j.ces.2004.01.070.

[66]   Y. Geng, D. Che, *Chem. Eng. Sci.* **2011**, *66* (2), 207–219. DOI: https://doi.org/10.1016/j.ces.2010.10.011.

[67]   D. Snider, S. Clark, P. O'Rourke, *Chem. Eng. Sci. - CHEM ENG SCI.* **2011**, *66*, 1285–1295. DOI: 10.1016/j.ces.2010.12.042.

[68]   T. Weinhart, C. Labra, S. Luding, J. Y. Ooi, *Powder Technol.* **2016**, *293*, 138–148. DOI: https://doi.org/10.1016/j.powtec.2015.11.052.

[69]   M. Sakai, S. Koshizuka, *Chem. Eng. Sci.* **2009**, *64* (3), 533–539. DOI: https://doi.org/10.1016/j.ces.2008.10.003.

[70]   Y. Liu, O. Hinrichsen, *Comput. Chem. Eng.* **2014**, *69*, 75–88. DOI: 10.1016/j.compchemeng.2014.07.002.

[71]   V. Verma, J. T. Padding, N. G. Deen, J. A. M. (Hans) Kuipers, F. Barthel, M. Bieberle, M. Wagner, U. Hampel, *AIChE J.* **2014**, *60* (5), 1632–1644. DOI: 10.1002/aic.

[72]   J. Chang, Z. Wu, X. Wang, W. Liu, *Powder Technol.* **2019**, *351*, 159–168. DOI: 10.1016/j.powtec.2019.04.028.

[73]   B. Hou, X. Wang, T. Zhang, H. Li, *Chem. Eng. J.* **2016**, *284*, 1224–1232. DOI: 10.1016/j.cej.2015.09.073.

[74]   M. S. Salehi, M. Askarishahi, H. R. Godini, R. Schomäcker, G. Wozny, *Ind. Eng. Chem. Res.* **2016**, *55* (5), 1149–1163. DOI: 10.1021/acs.iecr.5b02433.

[75]   C. Herce, C. Cortés, S. Stendardo, *Fuel Process. Technol.* **2017**, *167*, 747–761. DOI: 10.1016/j.fuproc.2017.07.003.

[76]   L. A. Vandewalle, G. B. Marin, K. M. Van Geem, *Energy & Fuels.* **2020**, *Accepted*. DOI: 10.1021/acs.energyfuels.0c02824.

[77]   D. Micale, R. Uglietti, M. Bracconi, M. Maestri, *Ind. Eng. Chem. Res.* **2021**, *60* (18), 6687–6697. DOI: 10.1021/acs.iecr.0c05845.

[78]   S. Jašo, H. Arellano-Garcia, G. Wozny, *Chem. Eng. J.* **2011**, *171* (1), 255–271. DOI: 10.1016/j.cej.2011.03.077.

[79]   Y. Simon, F. Baronnet, P. M. Marquaire, *Ind. Eng. Chem. Res.* **2007**, *46* (7), 1914–1922. DOI: 10.1021/ie060151w.

[80]   J. Sun, J. W. Thybaut, G. B. Marin, *Catal. Today.* **2008**, *137* (1), 90–102. DOI: 10.1016/j.cattod.2008.02.026.

[81]   H. Zanthoff, M. Baerns, *Ind. Eng. Chem. Res.* **1990**, *29* (1), 2–10. DOI: 10.1021/ie00097a001.

[82]   M. Maestri, D. G. Vlachos, A. Beretta, G. Groppi, E. Tronconi, *AIChE J.* **2009**.

[83]   M. Maestri, D. Livio, A. Beretta, G. Groppi, *Ind. Eng. Chem. Res.* **2014**, *53* (27), 10914–10928. DOI: 10.1021/ie501570b.

[84]   M. Bracconi, M. Maestri, A. Cuoci, *AIChE J.* **2017**, *63*, 95–104. DOI: 10.1002/aic.

[85]   S. B. Pope, *Combust. Theory Model.* **1997**, 41–63.

[86]   G. M. Goldin, Z. Ren, S. Zahirovic, *Combust. Theory Model.* **2009**, *13* (4), 721–739. DOI: 10.1080/13647830903154542.

[87] J. Li, B. Yang, *Chem. Eng. J.* **2018**, (xxxx), 1–10. DOI: 10.1016/j.cej.2018.08.204.

[88] S. Matera, M. Maestri, A. Cuoci, K. Reuter, *ACS Catal.* **2014**, *4* (11), 4081–4092. DOI: 10.1021/cs501154e.

[89] M. Bracconi, M. Maestri, *Chem. Eng. J.* **2020**, *400*, 125469. DOI: 10.1016/j.cej.2020.125469.

[90] M. Votsmeier, *Chem. Eng. Sci.* **2009**, *64* (7), 1384–1389. DOI: https://doi.org/10.1016/j.ces.2008.12.006.

[91] M. Votsmeier, A. Scheuer, A. Drochner, H. Vogel, J. Gieshoff, *Catal. Today*. **2010**, *151* (3), 271–277. DOI: https://doi.org/10.1016/j.cattod.2010.01.018.

[92] A. Scheuer, O. Hirsch, R. Hayes, H. Vogel, M. Votsmeier, *Catal. Today*. **2011**, *175* (1), 141–146. DOI: https://doi.org/10.1016/j.cattod.2011.03.036.

[93] M. Klingenberger, O. Hirsch, M. Votsmeier, *Comput. Chem. Eng.* **2017**, *98*, 21–30. DOI: https://doi.org/10.1016/j.compchemeng.2016.12.005.

[94] B. Partopour, A. G. Dixon, *Comput. Chem. Eng.* **2016**, *88*, 126–134. DOI: https://doi.org/10.1016/j.compchemeng.2016.02.015.

[95] B. Partopour, A. G. Dixon, *AIChE J.* **2017**, *63* (1), 87–94. DOI: https://doi.org/10.1002/aic.15422.

[96] J. E. Sutton, J. M. Lorenzi, J. T. Krogel, Q. Xiong, S. Pannala, S. Matera, A. Savara, *ACS Catal.* **2018**, *8* (6), 5002–5016. DOI: 10.1021/acscatal.8b00713.

[97] J. M. Lorenzi, T. Stecher, K. Reuter, S. Matera, *J. Chem. Phys.* **2017**, *147* (16), 164106. DOI: 10.1063/1.4997286.

[98] B. R. Goldsmith, J. Esterhuizen, J.-X. Liu, C. J. Bartel, C. Sutton, *AIChE J.* **2018**, *64* (7), 2311–2323. DOI: https://doi.org/10.1002/aic.16198.

[99] B. Partopour, R. C. Paffenroth, A. G. Dixon, *Comput. Chem. Eng.* **2018**, *115*, 286–294. DOI: https://doi.org/10.1016/j.compchemeng.2018.04.019.

[100] C. Stegelmann, N. C. Schiødt, C. T. Campbell, P. Stoltze, *J. Catal.* **2004**, *221* (2), 630–649. DOI: https://doi.org/10.1016/j.jcat.2003.10.004.

[101] K. B. and J. D. W. G. Froment, *Chemical Reactor Analysis and Design* **2011**.

[102] S. Rebughini, M. Bracconi, A. G. Dixon, M. Maestri, *React. Chem. Eng.* **2018**, *3* (1), 25–33. DOI: 10.1039/c7re00195a.

[103] M. Bracconi, Chem. Eng. Res. Des., 2022. DOI: https://doi.org/10.1016/j.cherd.2022.01.042.

Table and Figure Captions

Entry for the Table of Contents (Graphical abstract)

Computational Fluid Dynamics of Reacting Flows at Surfaces: Methodologies and Applications

D. Micale, C. Ferroni, R. Uglietti, M. Bracconi, M. Maestri*

Type of Article: Numerical methodologies and speed-up strategies for the multiscale investigation of catalytic processes are reviewed

Figure TOC